Khatawkar *et al.*
CABI Agriculture and Bioscience (2024) 5:80
https://doi.org/10.1186/s43170-024-00286-3

CABI Agriculture and Bioscience

RESEARCH

Open Access

Knapsack air assisted electrostatic sprayer for agricultural formulations

Dipak S. Khatawkar[1*], Dhalin Dharaneedharan[1] and P. Shaji James[1]

Abstract

An experimental prototype of a backpack-type rechargeable battery-powered air-assisted electrostatic sprayer was designed and tested for performance while preserving techno-commercial competence and affordability for India's marginal and small farmer communities. The designed prototype electrostatic sprayer achieved good levels of charge induction on the spray particles at various electrode potentials (1 to 12 kV). At a charging electrode potential of 9 kV and a nozzle discharge rate of 2 mL s^{-1}, electrostatically charged spray had a maximum charge to mass ratio (CMR) of 1.79 mC kg^{-1}. The Electric Ducted Fan (EDF) used for high velocity air assistance was capable of transporting charged spray droplets onto distant targets such as orchard trees and field crops with a spray throw of up to 5 m. The high-pressure atomization method produced fine droplets within a Volume Median Diameter (VMD) range of 90 to 100 µm, resulting in better charge induction and wrap-around effect. As the prototype features fewer moving mechanical components, reduced total noise and vibrations, it promises operator comfort in the long run while requiring less system maintenance. Environmental contamination can be minimized as the large quantity of harmful chemicals be prevented from drifting into the soil and nearby waterbodies. The competitive performance and lower investment could encourage majority of the Indian famers to upgrade with the developed air assisted electrostatic spraying system contributing to agro-socio-economic welfare.

Keywords Crop protection, Electrostatics, Environmental protection, Particle charging, Pest management, Spray drift

Introduction

Crops have been vulnerable to variety of pests and diseases from the time they were domesticated, resulting in yield losses that frequently threaten the global food security. Pre-harvest crop losses due to pests are between 10 to 28 per cent on a global scale for agricultural production (Savary et al. 2019). Pest-related losses to agricultural productivity alone were estimated to reach 42.66 million USD in India each year (Sushil 2016). Food and Agriculture Organization of the United Nations (FAO) estimates that annually up to 40 per cent of global crop production is lost to pests. Each year, plant diseases cost the global economy over 220 billion USD, and invasive insects at least 70 billion USD (IPCC 2021). For agriculture to be economically viable, to produce food at a reasonable cost, and to ensure an adequate food supply for the world's expanding population, plant protection is a necessity. Lack of proper pest and disease management, potential crop losses might reach up to 82 per cent (Oerke 2006).

Moreover, overwhelming post-harvest losses have been reported from the underdeveloped nations experiencing the worst cases. In addition to the losses, *mycotoxins* – the toxic secondary metabolite produced by fungi, can seriously endanger both human and animal health (Magan et al. 2011; Van Der FelsKlerx et al. 2016). The immense harm that pest outbreaks can do is evident from historical and contemporary examples.

Recently, the climate change induced pest outbreaks, especially of invasive insects have been on the rise in many parts of the world (IPCC 2021). One of the major

*Correspondence:
Dipak S. Khatawkar
dipakkhatawkar@gmail.com
[1] Department of Farm Machinery and Power Engineering, Kerala Agricultural University, Thrissur, India

problems being faced in vegetable cultivation is the invasive pest called Neotropical solanum whitefly (*Aleurothrixus trachoides*), which is spreading fast in South India (Sundararaj 2018). The peculiarity of the pest is its leaf-underneath habitat on the host crop mainly brinjal, chilly and tomato. The conventional application methods can deposit the pesticide on the top surface of plant leaves only and found to be obsolete in controlling invasive pests like whitefly (Latheef et al. 2008). Whereas the electrostatic spray technique is well known for its wrap-around effect which could effectively deposit the pesticide spray on the upper as well as leaf underneath surfaces where the target pest inhabits (Patel et al. 2015). It can also improve the deposition efficiency by about 80 per cent with 50 per cent or lesser spray chemicals. At present, a number of electrostatic spraying systems are commercially available worldwide and mainly manufactured by United States (ESS®-MaxCharge™), Italy (Martignani Inc.) and China (Henan Yugong Machinery Pvt. Ltd.) based firms. However, the marginal farmer community in India is reluctant to own such a technologically advanced plant protection equipment, even though being effective, due to their high costs.

Lin et al. (2023) reported that, the traditional spraying technology is ineffective for agricultural plant protection in small plots due to its poor droplet refining ability, short spraying area, high pesticide consumption, and high manual spraying cost. Spraying pesticides is currently the primary method of preventing crop diseases and insect pests from spreading. The integration of an agricultural plant protection vehicle with electrostatic spray technology could solve spraying efficiency, droplet adsorption rate, and evenness issues. Improving the effectiveness of plant protection and pesticide application is critical.

An attempt was made to address and fulfill this techno-economic gap with a holistic approach and this paper is a result of an exhaustive process of design and development of an affordable backpack type battery powered air assisted electrostatic induction sprayer for agricultural applications.

Materials and methods

Design considerations for the development of electrostatic induction spray charging system

The method of electrostatic induction spray charging was adopted for this study by considering its known advantages over other charging methods such as high charge transferability, less hazardous to life and simplicity in construction (Law 1975; Lane and Law 1982). The airborne particles those can be significantly guided by dielectrophoretic forces of spatially divergent fields, necessarily should have the essential condition for electrical force management is,

$$F_p = q_p \cdot E \tag{1}$$

where, F_p is the electrical force (N) experienced by an individual particulate, q_p is the net unipolar charge (C) on the particulate, and E is the electric-potential gradient (V m^{-1}) existing at the location of the particle formation zone. This driving electric field may commonly result from: (a) conveniently positioned high-voltage electrodes; (b) induced image charges in nearby grounded boundaries; and from (c) electric space-charge fields generated by nearby airborne assemblies of other charged particles, including the charged cloud in which the individual charged particulate resides.

Criteria for introducing an electric field to liquid droplets

In theory, the level of droplet charge (q_p) imparted by the electrostatic induction process should depend profoundly upon the relative time rate of charge transfer to the droplet-formation zone as compared with the time required for droplet formation.

In terms of the liquid's dielectric constant (κ), permittivity of air (ε_0) and resistivity (ϱ), the time constant becomes,

$$\tau = \kappa \times \varepsilon_0 \times \varrho = 76.546 \times 8.85 \times 10^{-12} \times 2 \times 10^2 = 1.3548 \times 10^{-7} s \tag{2}$$

(For water κ = 76.546 F m^{-1} at 30°C, for air $\varepsilon_0 = 8.85 \times 10^{-12}$ $C^2 \cdot N^{-1}$ m^{-2} and $\varrho = 2 \times 10^2$ Ω m).

Theoretically, a spray liquid having charge transfer time constant (τ) is less than the length of time t_f (s) which characterizes droplet formation, should be compatible with the electrostatic induction charging process. Whereas, the liquids having $\tau > t_f$ could not satisfactorily be charged by the method of electrostatic induction (Law 1975).

The generalized schematics of electrostatic induction charger as shown in Fig. 3a illustrates geometric arrangement of components, for which the characteristic expression for droplet-formation time is,

$$t_f = \frac{l_c}{v} \tag{3}$$

where, l_c (m) is the horizontal length of liquid sheet cylindroid and v is the velocity of flow (m·s^{-1}). At operating pressure of 6 kg cm^{-2}, nozzle orifice diameter of 0.5 mm and measured discharge rate (Q) of 2 mL s^{-1}, velocity of flow (v) was found to be 10.19 m s^{-1}. Therefore, the characteristic droplet formation time or phase transition time was calculated as,

$$t_f = \frac{1.2 \times 10^{-2}}{10.19} = 1.1776 \times 10^{-3} s \quad (4)$$

Therefore, the essential theoretical requirement to impart the unipolar charge on liquid particulates by electrostatic induction, $\tau << t_f$ was satisfied.

Prediction of spray cloud current

For $\tau << t_f$ the electrostatic induction charging system as illustrated in Fig. 1 could be approximated by two coaxial conducting cylinders in order to predict the electric field strength at the droplet formation zone, the charge density on the liquid sheet surface and the total droplet current. The electric field intensity (*Ej*) just off the surface of the liquid sheet cylindroid of radius r_c (m) where droplet formation commenced. This could be approached as a function of outer cylinder (charging electrode) radius r_e (m) and applied potential difference V by the field equation for concentric conducting cylinders of infinite length (Law 1975) as,

$$E_j = \frac{V}{r_c \ln(\frac{r_e}{r_c})} V \cdot m^{-1} \quad (5)$$

By Gauss' law the free surface charge density ρ_s (C m^{-2}) on the liquid sheet cylindroid would be,

$$\rho_s = \varepsilon_0 \times E_j C \cdot m^{-2} \quad (6)$$

Thus, the expected spray-cloud current i_c (A) carried by the charged liquid would be,

$$i_c = 2\pi r_c \cdot \varrho_s \cdot \nu \quad (7)$$

In terms of the applied charging voltage (V) and the liquid flow velocity (ν) (m s^{-1}) this prediction equation for spray-cloud current becomes,

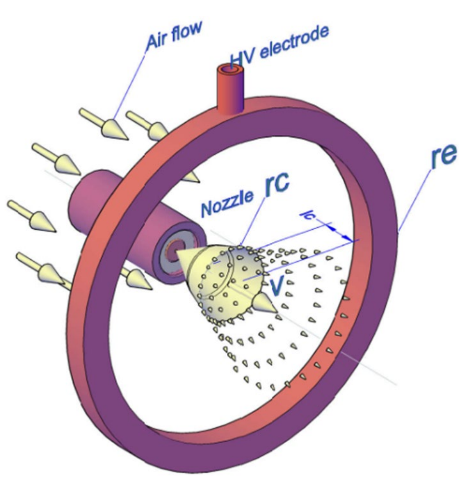

Fig. 1 Comprehensive electrostatic induction spray charging system

$$i_c = \frac{2\pi \cdot \varepsilon_0 \cdot V \cdot \nu}{\ln(\frac{r_e}{r_c})} \quad (8)$$

From the observed Volume Median Diameter (VMD or D_{V50}), the droplet charge could be predicted theoretically by,

$$q_p = \frac{30\varepsilon_0 \cdot r_p \cdot V}{\ln(\frac{2r_e}{r_p})} C \quad (9)$$

From the value of D_{V50}, volume (V_{DV50}) and thereby mass (m_p) of the spherical particle could be calculated,

$$V_{DV50} = \frac{4}{3} \times 3.14 \times (r_p)^3 m^3 \quad (10)$$

Since, the mass density of water (ρ_w) is 997 kg m^{-3}, mass of the droplet could be estimated as,

$$m_p = \rho_w \cdot V_{DV50} kg \quad (11)$$

Therefore, charge-to-mass ratio (CMR, mC kg^{-1}) could be predicted by,

$$CMR_{theoretical} = \frac{q_p}{m_p} mC.kg^{-1} \quad (12)$$

Charging efficiency of electrostatic induction charger

Performance of an electrostatic particulate charging system in terms of charging efficiency is determined by comparison of the imparted particulate charge to the maximum theoretical charge limit. For the agricultural airborne liquid particles having surface tension values (Γ, N m^{-1}) typical of water ($\Gamma = 71.99 \times 10^{-3}$ N m^{-1}) and common pesticides, this limit is influenced by hydrodynamic instability and rupture of the surface of the droplets due to repulsive force between unipolar charges, called Rayleigh limit. Therefore, for any given liquid particle a maximum surface charge density value (ρ_s) exists such that the outward expanding electrical force (due to repulsive nature of unipolar charges) on the liquid surface is just balanced by the restraining force of surface tension. The value of maximum droplet charge limit (q_{max}) could be calculated as,

$$q_{max} = 8\pi \sqrt{\varepsilon_0 \cdot \Gamma} \cdot (r_p)^{3/2} \quad (13)$$

Charging efficiency of an electrostatic induction spray charging system is defined as the percentage of maximum droplet charge or CMR achieved. The ratio of the charge imparted practically on a droplet to the maximum droplet charge or maximum CMR at Rayleigh limit is given by the equation:

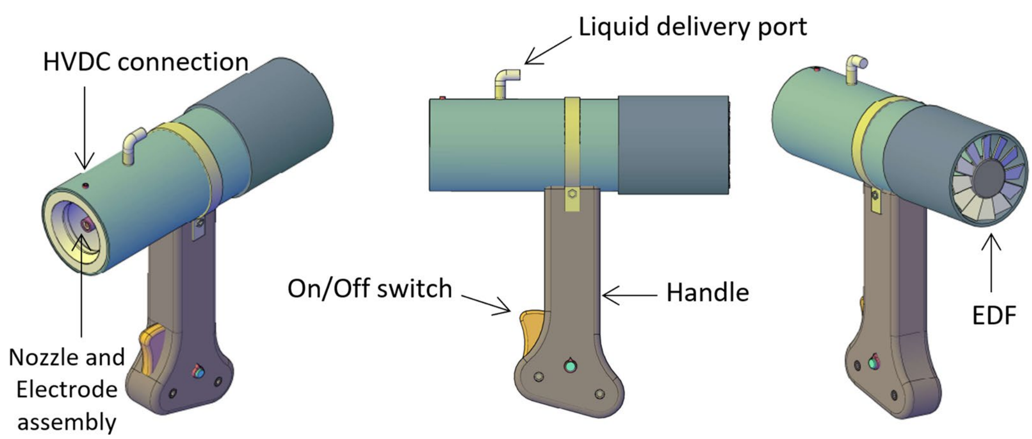

Fig. 2 Conceptual design of handheld electrostatic spray gun

$$Chargingefficiency(\%) = \frac{CMR_{Achieved}}{CMR_{Rayleigh\ limit}} \times 100 \quad (14)$$

Spray droplet size and deposition analysis

Deposition characteristics were primarily dependent on effective droplet diameter (VMD and NMD). The droplet spectra were captured on the water sensitive papers using aqueous spray solution and scanned images were then analyzed using USDA's 'DepositScan' Program in ImageJ image processing computer software. The results from the analysis were filtered out in terms of droplet size distribution (DV_{10}, DV_{50} and DV_{90}) representing the distribution of the droplet diameters such that the droplets with a diameter smaller than DV_{10}, DV_{50} and DV_{90}, composed 10, 50 and 90 per cent of the total spray volume. With the gentle (to minimize impact spreading) blower speed of 1.0 m s^{-1}, spray nozzle was operated with three different pressures (4.0, 5.0 and 6.0 kg cm^{-2}) to determine the optimum working pressure to produce finer droplet spectra. Also, the effect of electrostatic charging on droplet size and distribution was accounted and compared with the developed spray system without electrostatic charge.

Uniformity coefficient (UC)

Uniformity coefficient is the ratio of VMD to NMD, a factor used for indicating the uniformity of the spectra. The VMD is affected by relatively few large droplets whereas the NMD is more influenced by small droplets. The more uniform the spray spectra, the closer the ratio of VMD and NMD approaches to unity.

$$U_C = \frac{VMD}{NMD} \quad (15)$$

Relative span (RS)

Relative span refers to a spray quality indicator determined by subtracting the DV_{10} value from the DV_{90} value and dividing by the DV_{50}. The numerical value of R_S describes the width of the particle size distribution curve plotted against the frequency of occurrence. The smaller R_S, lesser is the variation between the sizes of the droplets in the spray spectrum.

$$R_S = \frac{DV_{90} - DV_{10}}{DV_{50}} \quad (16)$$

Results and discussion

The salient results of the investigations taken up to develop an electrostatic induction charging system and a liquid atomizer compatible to a DC power to aid electrostatic spraying is elucidated in this section. The results of the laboratory experiments conducted during the development of this battery-operated electrostatic spraying system are also discussed here. An electrostatic spray charging unit (ESCU) was developed based on electrical design principles and had a variable high voltage power module, a hydraulic atomization system and a blower for the high velocity air assistance main components (Fig. 2).

Electrostatic induction spray charger

The nozzle employed in the system produced infinitesimally small free jet length just off the nozzle orifice (0.5 mm) and observed to be instantaneously diverging into a hollow cylindroid liquid sheet. The length of the cylindroid liquid sheet at the operating pressure 6 kg·cm^{-2} was observed to be 12 mm, measured horizontally from the centre of nozzle orifice. The diameter at the terminal point of the cylindroid was measured to be 10 mm, thereafter liquid sheet commenced to breakup into ligaments and consequently into tiny droplets due to hydrodynamic instability. The nozzle discharge (Q) measured using graduated measuring cylinder and corresponding velocity of flow (v), was found out as 2 mL s^{-1} and 10.19 m s^{-1} respectively. The electric field intensity (E_j) induced by the charging electrode (r_e = 27 mm) at the liquid sheet cylindroid surface of radius r_c = 5 mm determined on the basis of generalized coaxial conductive cylindrical capacitor geometry, was found to be 1.0675×10^6 V m^{-1}.

The major requirement in liquid particulate charging by induction method was $\tau < t_f$ and for the developed induction charger system, transfer time constant ($\tau = 1.3548 \times 10^{-7}$ s) was found to be much lesser than droplet formation time ($t_f = 1.1776 \times 10^{-3}$ s). This enabled the electrostatic induction spray charging system to induce a substantial image charge on the liquid spray particulates emerging through droplet formation zone successfully. The free surface charge density (ρ_s) on the liquid sheet cylindroid due to induced static electricity was found to be 9.4473×10^{-6} C m^{-2} and the analogous spray-cloud current i_c (A) carried by the charged liquid was mathematically predicted to be 3.0228 μA. Another prediction on the basis of applied charging potential (+9 kV) and the liquid flow velocity (10.19 m s^{-1}) led the spray cloud current to the value of 3.0224 μA (Fig. 2).

Variable high voltage power supply

A dc-dc high voltage generator module consisting Power MOSFET (IRFZ44N) driver circuit, Pulse Width Modulator (PWM) and Line Output Transformer (LOPT or flyback) was developed to output variable high voltage up to 12 kV DC with standard 18,650 rechargeable Lithium-ion battery pack (3.7 V DC, 12,000 mAh) (Dwivedi and Daigavane 2011; Choi et al. 2016). High voltage polymer capacitors (2 kV DC, 10 nF) in series were connected across the output high tension terminals of the LOPT as a filter the ripple and to handle the accidental loading (Sharma et al. 2015; Waluyo et al. 2015; Patel et al. 2014; Petersen 1989).

High voltage electrode assembly

The high voltage charging ring electrode (5 mm thickness, 54 mm diameter, material—copper) was housed inside an external groove on a cylindrical sleeve fabricated using cast nylon material (Fig. 3). The outer diameter of the electrode carrier sleeve was 73 mm and a gentle gradient was given to the internal surface of the sleeve using taper turning. The converging gradient to the inner surface was provided to increase the air velocity at point where charging electrode and droplet formation zone were located. This ensured that electrode carrier assembly would not retain the tiny droplets due to electrostatic attraction and free of resultant short circuit between nozzle and charging electrode.

The intake side of the electrode carrier was having internal diameter of 70 mm and 51 mm on exit side. The cast nylon material with a dielectric strength of 19.7 kV·mm^{-1} exhibited necessary electrical insulation.

Since, the electrode carrier sleeve was designed and fabricated to fit inside the air blower conduit made of PVC (wall thickness = 2.5 mm, dielectric strength = 14 kV·mm^{-1}), the high potential electrode was thus insulated from all the sides. This electrically secured geometry was meant to avoid accidental human contact

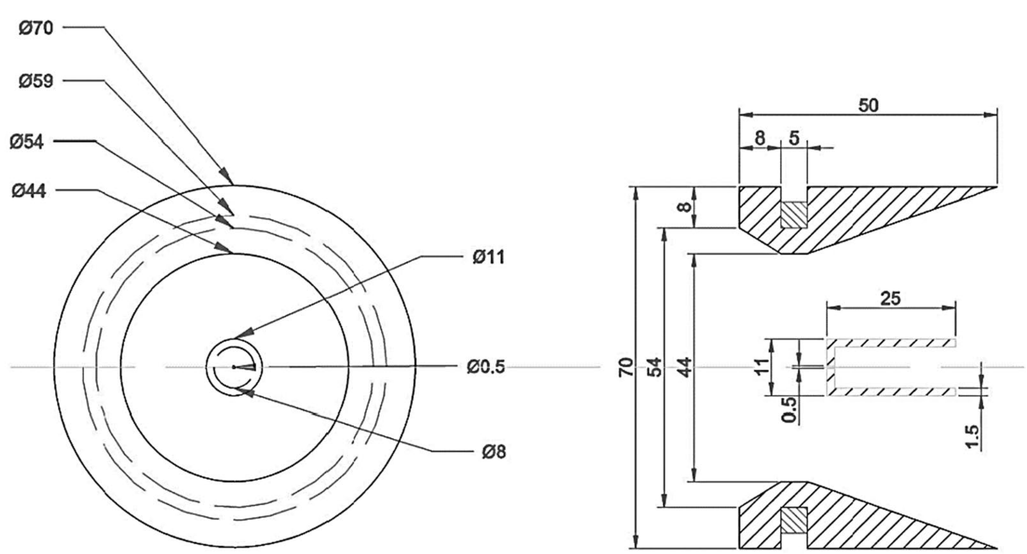

Fig. 3 Constructional details of electrode carrier sleeve (all dimensions are in mm)

with the high voltage electrode and corrosion of the electrode material due to chemical action and environmental impact.

Atomization and nozzle characteristics
The spay nozzle was operated at different pressures (4, 5 and 6 kg cm^{-2}) using dual channel differential valve to observe the spray droplet spectrum. The range of droplet size (VMD = 90 to 100 μm) observed at 6 kg cm^{-2} was finest possible as compared to droplet size observed at 4 kg cm^{-2} (170 to 180 μm) and 5 kg cm^{-2} (135 to 155 μm). The droplet spectrum obtained at 6 kg·cm^{-2} operating pressure was the only sub-100 μm facilitating better spray chargeability longer terminal time (Almekinders 1992). Hence, the hydraulic nozzle was assessed for the spray characteristics. The cone angle was found to be 60° at operating pressure of 6 kg cm^{-2} with the spray swath measured to be 650 mm, when nozzle was operated vertically downwards at an elevation of 700 mm above the flat surface. The volumetric discharge of the selected spray nozzle was measured to be 2 mL s^{-1}.

High speed air blower unit
An Electric Ducted Fan (EDF) was selected as the main component to develop the high-speed air blower. The internal diameter of the ducted fan was 70 mm with 12 blades mounted on DC synchronous permanent magnet motor with KV1850 rpm rating. The motor was driven by the Universal Battery Eliminator Circuit (UBEC) integrated with Electronic Speed Controller (ESC) which could be operated with 7.5 to 25 V DC power supply. The maximum air discharge from the EDF at full throttle was recorded as 0.088 m^3 s^{-1} with an air delivery speed of 23 m s^{-1}.

Light weight backpack assembly
In order to keep the overall weight of the sprayer as low as possible, a compact backpack frame was fabricated using 25 mm CPVC tubes with three horizontal compartments. The compartments were made using PVC board of 3 mm thickness. The lower compartment accommodated the battery, diaphragm pump and the pressure control system.

The developed battery powered electrostatic sprayer comprised of two units viz. handheld electrostatic spray gun and backpack assembly. The spray nozzle, embedded charging electrode assembly, EDF and the handle grip were the components of developed handheld electrostatic spray gun. While, the backpack assembly comprised of the spray solution tank, HVDC power supply, battery, diaphragm pump, control valve and the pressure gauge. The developed prototype weighed about 10 kg (dry weight). The various components of the developed battery powered backpack type electrostatic sprayer are described Fig. 4.

Analysis of spray droplet spectrum
The volumetric distribution of the spray droplet spectrum revealed that volume median diameter (VMD or DV_{50}) of the spray was 91 μm, while DV_{10} = 60 μm and DV_{90} = 116 μm as illustrated in Fig. 5. Also, the number median diameter was (NMD) found to be 67 μm, which was when related to the VMD, resulted in the uniformity coefficient (UC) of 0.73. Also, the relative span (RS) of the spray spectrum was found to be 0.61.

The spray droplet spectrum was analyzed for the frequency distribution for individual class and cumulative frequency as illustrated in Fig. 6. The maximum frequency was observed for the droplet size class of 61 to 70 μm, followed by class of 51 to 60 μm. The droplet size ranging between 51 to 80 μm covered the 2/3rd portion of the frequency distribution, whilst the range of droplet size 81 to 120 μm contributed only 1/3rd to the total distribution (Fritz et al. 2009; Jaworek et al. 2009).

Measurement of spray cloud current
The developed electrostatic induction spray charging system was assessed for its effective spray chargeability with respect to different levels of charging electrode potentials and assisting air velocity at constant nozzle discharge.

Calculation of charge to mass ratio (CMR)
The observed Volume Median Diameter (VMD or D_{V50}) was 91 μm and the charge carried by a droplet (q_p) could be predicted theoretically as 1.539×10^{-11} C. The ratio of droplet charge and mass of the droplet gave the theoretical CMR to the value of 42.90 mC kg^{-1}.

However, the threshold value of CMR that could be attained practically given by Rayleigh limit (q_{max}) was found to be 15.56 mC kg^{-1}, by considering the agricultural airborne liquid particles having surface tension 71.99×10^{-3} N m^{-1} and permittivity of air 8.85×10^{-12} C^2 N^{-1} m^{-2} at 30°C.

Spray charging capacity of the developed electrostatic spray charger
Spray cloud current measurement was essential to validate and quantify the performance of the developed spray charging system. In the laboratory experimental setup, the spray cloud current was measured using charge collector device coupled with digital multimeter, which was recorded to the maximum value of 3.3 μA at charging electrode potential of 9 kV. The charge to mass ratio was determined by taking ratio of the measured constant spray cloud current (2.5 μA) and the collected mass of spray liquid with respect to time (1.4 mL s^{-1}).

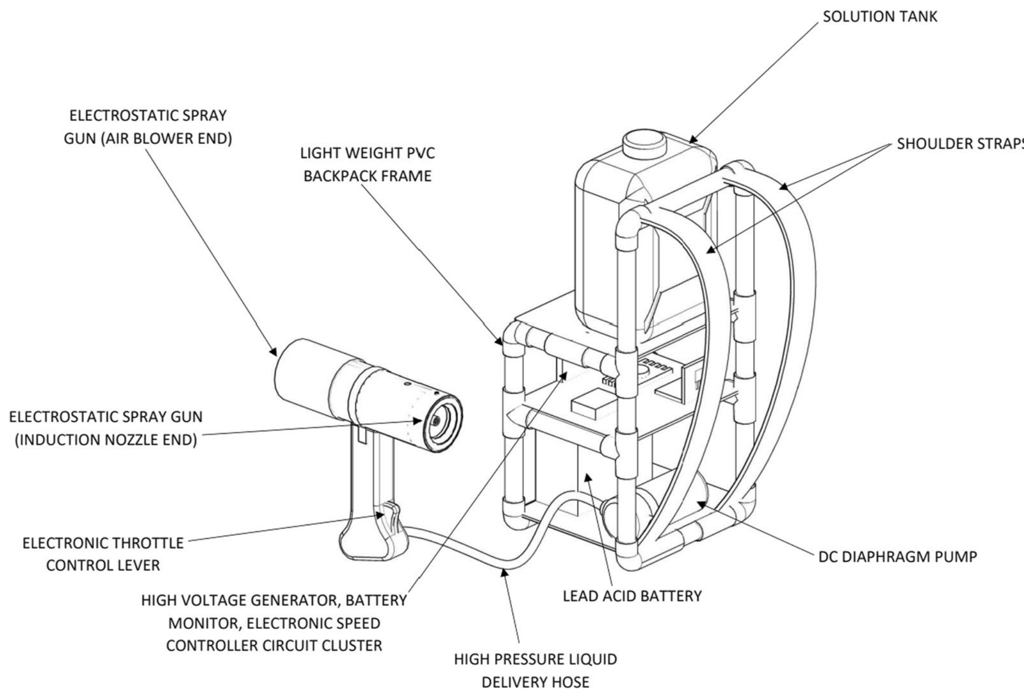

Fig. 4 CAD of developed electrostatic sprayer

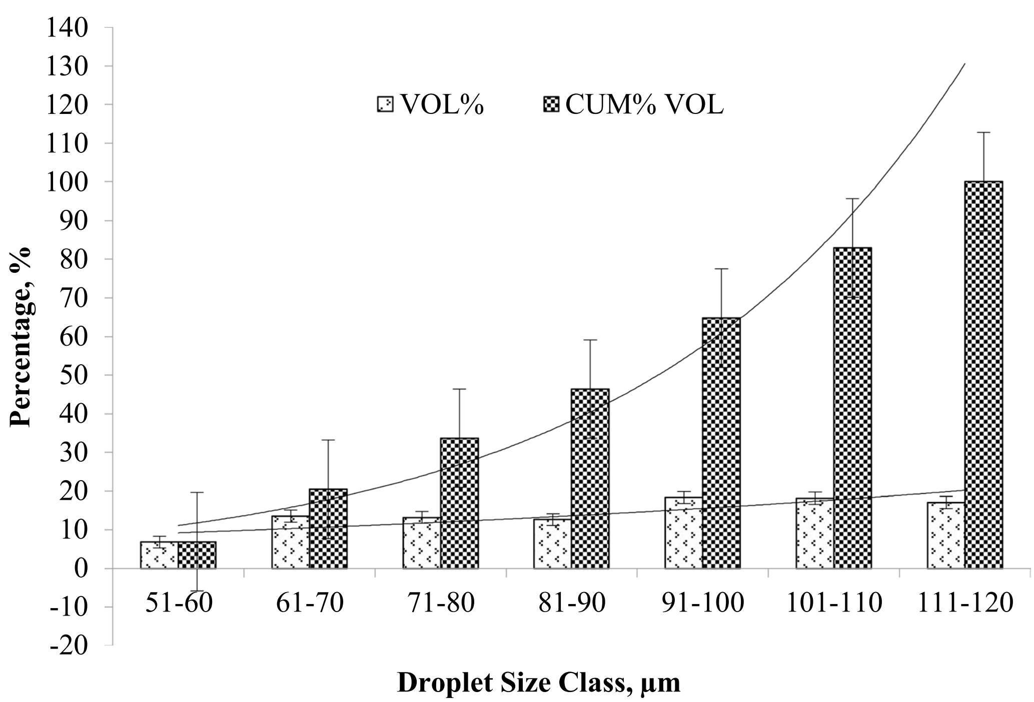

Fig. 5 Volumetric distribution of spray droplet spectrum

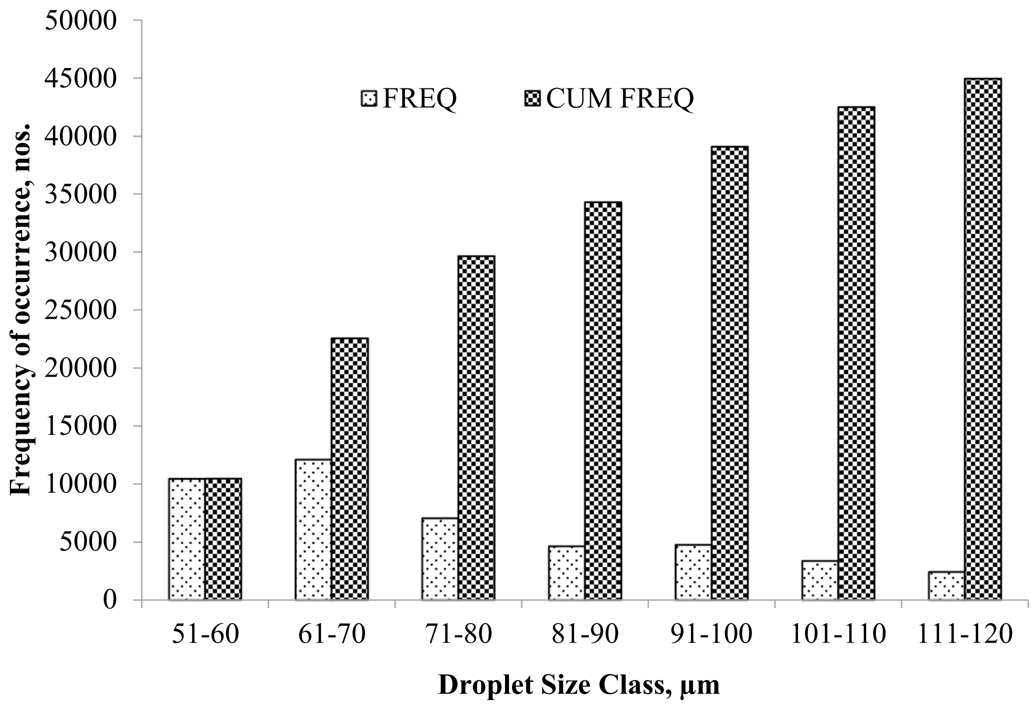

Fig. 6 Frequency distribution of spray droplet spectrum

The maximum CMR level practically achieved was 1.79 mC kg^{-1}, similar to the spray chargeability reported (2.35 mC kg^{-1}) by Yu et al. (2011) and (0.37 mC kg^{-1}) Mamidi et al., (2012) respectively.

Effect of charging electrode potential on CMR

The spray cloud current and in turn the CMR was observed to be increasing from 0.46 to 1.79 mC kg^{-1} with increase in electrode potential from 1 to 9 kV respectively at an air velocity of 10 m s^{-1}. However, further increment in the electrode potential from 9 to 12 kV resulted in abrupt fall in the CMR value from 1.79 to 0.61 mC kg^{-1}. This could be the result of reverse ionization and wetting of electrostatic spray gun due to excessive electrode potential (Bode and Bowen 1991; Alamuhanna and Maghirang 2010).

The trajectory of emerging spray particles might have been so influenced due to excessive electrode potential that they were been driven back towards the electrode. The deposition of tiny spray liquid particles onto the charging electrode assembly hindered the process of electrostatic charge induction which in turn could be the cause of abrupt decline in the CMR beyond the electrode potential of 9 kV.

The results obtained from the experimental data were statistically analyzed and reported in terms of analysis of variance (ANOVA) using R-studio, an open-source computer environment based on R-language and Tukey-HSD (Honestly Significant Difference) test was conducted for comparison of means.

Statistical analysis (Table 1) revealed that, the developed electrostatic spray charging system generated maximum CMR of 1.79 mC kg^{-1} at 9 kV which was significantly superior to all other electrode potential levels followed by 8 kV and 7 kV and vice versa.

Table 1 Tukey-HSD test for effect of electrode potential on CMR

Sl. No	Electrode potential, kV	Mean CMR, mC kg^{-1}
1	V_9	1.79^{a}
2	V_8	1.61^{b}
3	V_7	1.57^{c}
4	V_6	1.50^{cd}
5	V_{10}	1.43^{cd}
6	V_5	1.28^{de}
7	V_{11}	1.28^{de}
8	V_4	1.07^{e}
9	V_3	0.71^{f}
10	V_{12}	0.61^{f}
11	V_2	0.61^{f}
12	V_1	0.46^{f}

Significance level, α = 0.05; The superscripts (a to f) are designated in alphabetic series according to the similarity/dissimilarity between Mean CMR values and thereby exhibiting quantitative distinctions

Effect of assisting air velocity on CMR

The spray assisting air velocity was observed to be influencing the spray chargeability of the electrostatic induction charger (Celen et al. 2009). The CMR value of charged spray followed the increasing trend with the increase in the assisting air velocity. The CMR of the charged spray at optimum charging potential (9 kV) increased respectively as 1.15 mC kg^{-1}, 1.54 mC kg^{-1} and 1.79 mC kg^{-1} with respect to the air assistance velocity of 5 m s^{-1}, 7.5 m s^{-1} and 10 m s^{-1}.

The gradual improvement in the CMR value at a constant electrode potential and incremental air velocity might have expedited the spray particles to escape swiftly through the strong electrostatic field inside the spray charging gun (Maynagh et al. 2009; Robson et al. 2013). This could be the reason behind enhanced spray chargeability without excessive wetting of charging electrode.

Charging efficiency of the developed electrostatic spray charger

The charging efficiency of the developed electrostatic induction spray charging system at maximum CMR of 1.79 mC kg^{-1} observed in terms of percentage of Rayleigh charge limit (15.91 mC kg^{-1}) achieved was found to be 11.25 per cent at electrode potential of 9 kV.

Deposition characteristics

Adaxial and abaxial deposition

The image processing analysis revealed that, there was approximately three-fold increase in the spray deposits per square centimetre of average leaf top surface area with electrostatically charged spray (327 deposits cm^{-2}) compared to conventional knapsack sprayer (102 deposits cm^{-2}). The existence of prominent electrostatic wrap-around effect was observed validated the successful charge induction on spray droplets (Gaunt et al. 2003; Antuniassi et al. 2011; Zhou et. al. 2024). When the charging system was activated, a good extent of deposition on the underneath leaf surface was observed (Figs. 7 and 8). The average droplet population on the surface was observed to be 250 droplets per cm^2. In both the cases of developed spraying system without electrostatic charging and conventional manually operated knapsack sprayer, no deposition on abaxial leaf surface was observed. The conventional sprayer executed excess deposition on adaxial leaf surface which caused undesirable dripping of applied spray solution.

Deposition efficiency

The spray deposit distribution of electrostatic spray was accounted in terms of percentage of total spray volume applied as 50.62 per cent on-target, 10.09 per cent on ground and 39.27 per cent in the form drift compared to

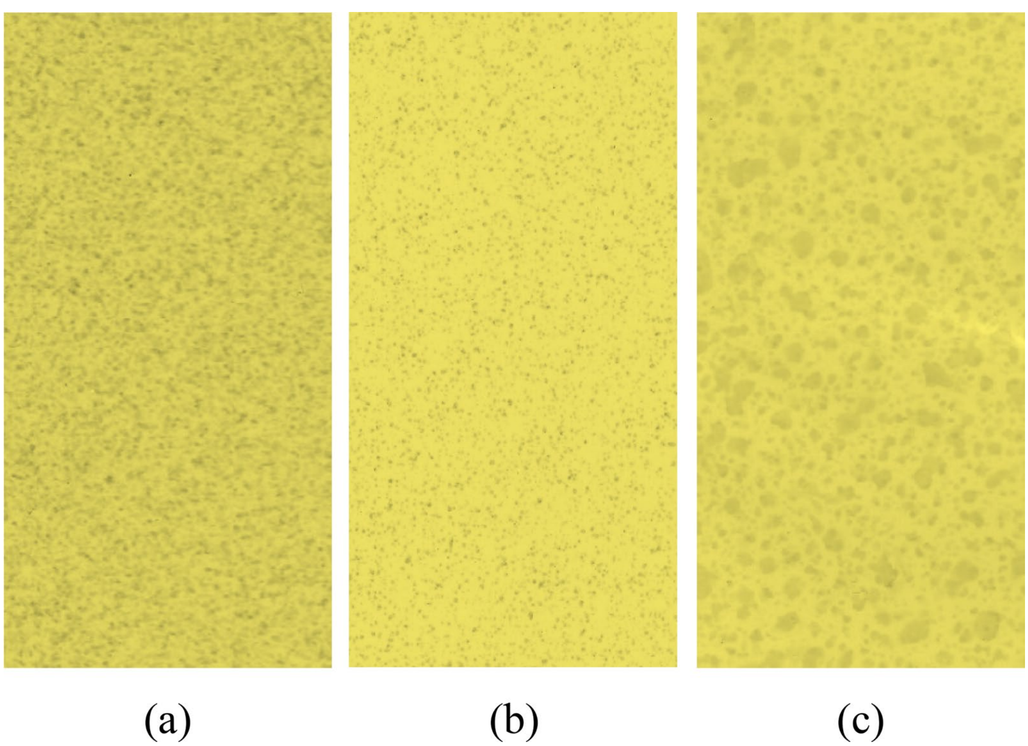

Fig. 7 Adaxial deposition (**a**) Electrostatic, (**b**) Uncharged and (**c**) Conventional spray

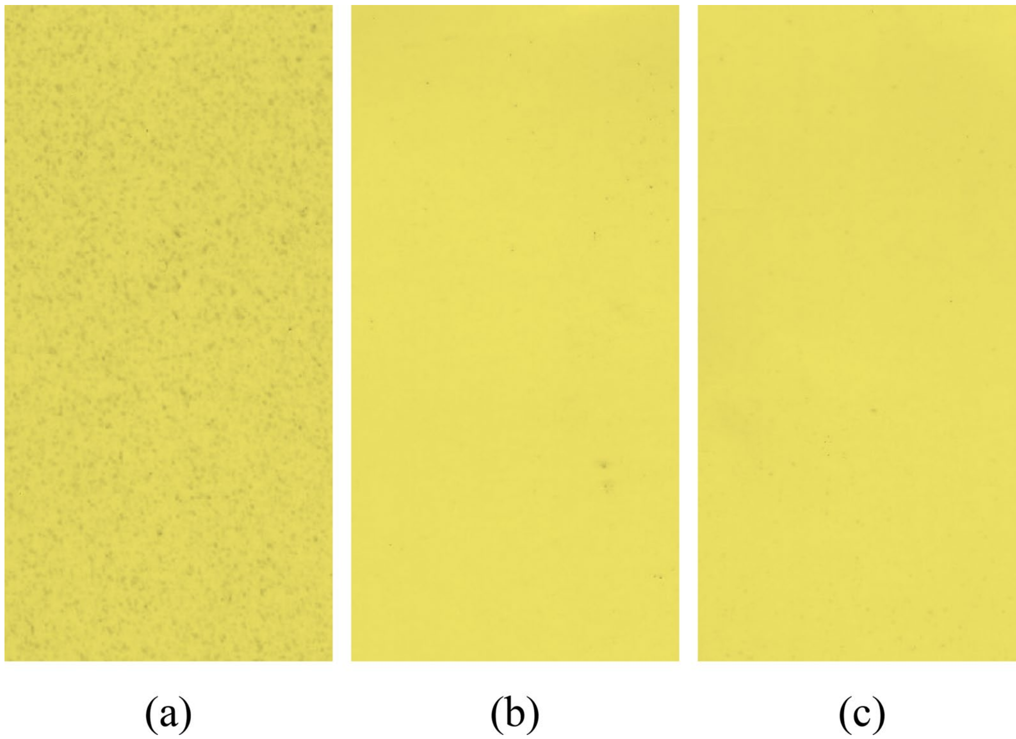

Fig. 8 Abaxial deposition (**a**) Electrostatic, (**b**) Uncharged and (**c**) Conventional spray

the conventional knapsack sprayer with corresponding percentage distribution as 28.20, 34.81 and 36.97 per cent respectively (Fig. 9).

It was clearly observed that the electrostatic spray charging improved the on-target deposition by 1.8 times than that of conventional spraying (Law and Scherm

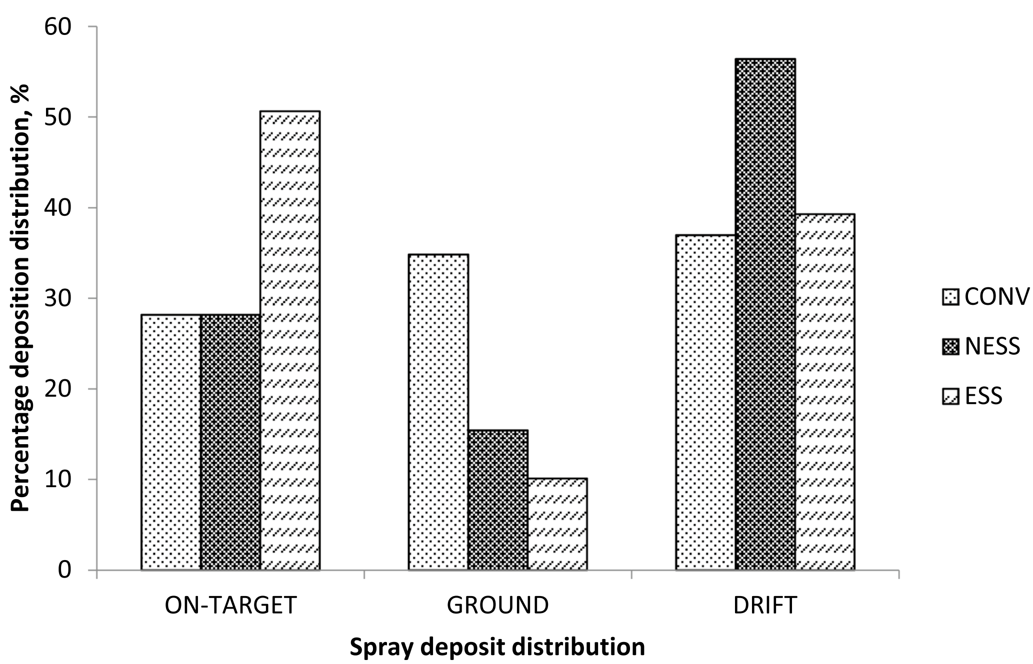

Fig. 9 Comparison of applied spray volume distribution

2005; Law and Cooper 1988). However, the developed spraying system without electrostatic charge resulted in the excess ground (15.41%) and drift (56.40%) losses resulted in on-target deposition of 28.19%. The excess off-target movement of applied spray volume might have occurred due to finer droplet spectra which was vulnerable to wind drift in absence of directorial electrostatic force (Esehaghbeygi et al. 2010).

Effect of canopy location on spray deposition

Approximately three-fold increment in upper canopy deposition was observed with electrostatically charged spray particles (350 deposits cm^{-2}) as compared to conventional spraying method (100 deposits cm^{-2}). Similar trend was observed in the cases of middle and lower canopy depositions (Appah et al. 2019; Barbosa et al. 2009). However, the abaxial leaf surface deposition in case of charged spray was found to be decremented when analyzed for upper (300—350 deposits cm^{-2}), middle (200—250 deposits cm^{-2}) and lower canopy (50—100 deposits cm^{-2}) leaves respectively.

Leaf area index (LAI)

The average Total Leaf Area per Plant (TLAP) and corresponding Plant Canopy Area (PCA) were measured using EasyLeaft image analysis software. These values were found to be 6425.45 cm^2 (Fig. 10) and 3894.21 cm^2 (Fig. 11) respectively. The average leaf area index (LAI) was observed to be 1.65 for brinjal crop and sprayer was calibrated to cover the 1 ha of the crop with 150 L of spray solution on the basis of existing practice of applying spray solution at the rate of 500 L ha^{-1}. Moreover, the computer-based image analysis process provided a non-destructive method to measure TLAP and PCA. The assessment revealed that the developed electrostatic spraying reduced the water requirement for spraying per unit area by 1/3rd, which could save tremendous amount of water being utilized in conventional methods of agricultural spraying.

Pesticide residue analysis

The fruit and leaf samples from the treated plants were collected on zeroth, third, fifth and seventh day of spray application. The standard method of chemical extraction was followed in order to determine the pesticide residues in the plant body using GC-ECD Gas Chromatograph – Electron Capture Detector (Agilent Technologies). The results were compared between the above spray treatments to quantify the field performance of the developed spraying system.

The results obtained from GC-ECD technique shown that, in spite of large spray volume (500 L ha^{-1} @ 1.5 mL L^{-1}) was being used to cover the crop canopies using conventional sprayer, the average content

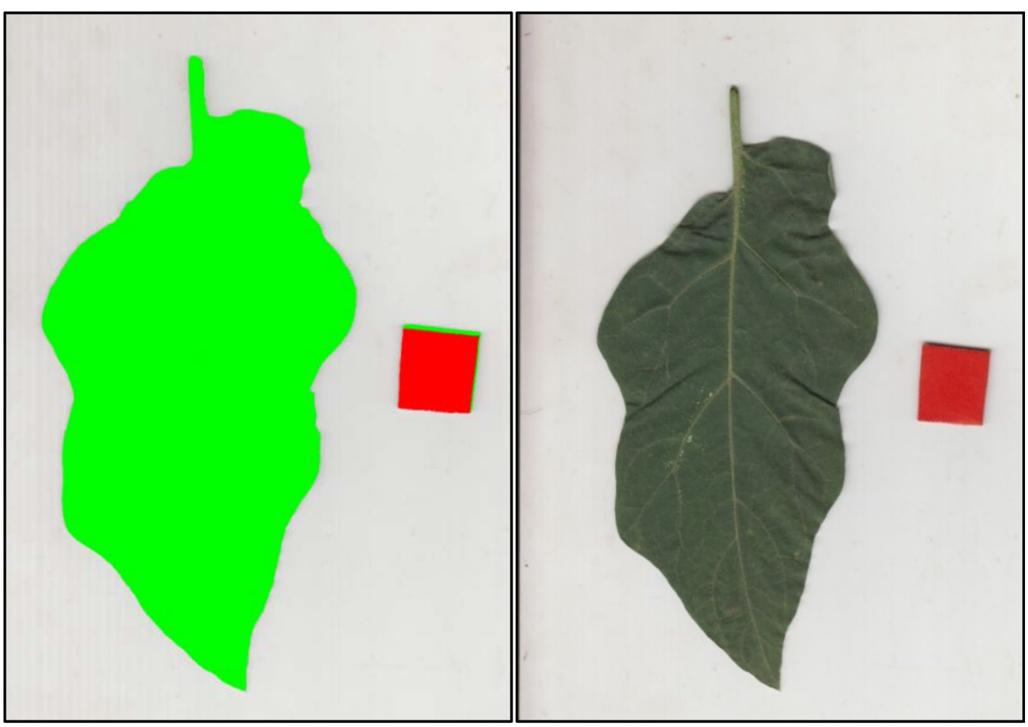

Fig. 10 Image analysis for measurement of individual leaf area using EasyLeaf software

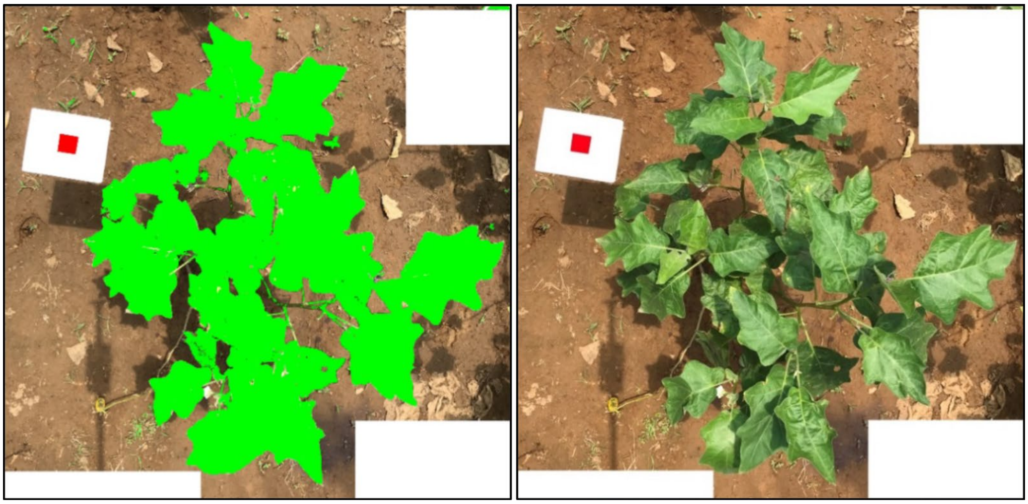

Fig. 11 Image processing of plant canopy area using EasyLeaf software

of active ingredient (47.37 ng μL^{-1}) found in the plant body samples was much lesser than that of achieved using electrostatic spraying (147.63 ng·μL^{-1}) with the same dose of active ingredient per hectare (150 L ha^{-1} @ 5 mL L^{-1}).

There was nearly about three-fold increase observed in the active ingredient (pesticide residue) present in the plant body on the day of spray application (Mishra et al. 2014; Tong-Xian et al. 2004). Even with the reduced dosage of active ingredient (3 mL L^{-1}), developed electrostatic spraying resulted in 44.38 per cent increase of pesticide residue in the samples compared to conventional spraying method (Luciana and Cramariuc 2009; Asano 1999).

In the case of conventional spraying, GC-ECD analysis of the plant body samples collected on subsequent days shown that gradual reduction in the pesticide residue reached to null point on 5th day after spray application. On the other hand, electrostatic spraying had shown 44.53 ng μL^{-1} and 16.93 ng μL^{-1} pesticide residues on 5th and 7th day respectively.

The longer residence of pesticide residue on the target plant could help the electrostatic spraying treatment to control the pest activity superior over the conventional spraying method (Salcedo et al. 2023; Gil et al. 2011). Figure 12 illustrates the residual pesticide content observed for different spray treatments viz. T_1—Conventional high-volume sprayer (1.5 mL L^{-1}) 500 L ha^{-1}, T_2—Electrostatic sprayer (5 mL L^{-1}) 150 L ha^{-1}, T_3—Non-electrostatic sprayer (5 mL L^{-1}) 150 L ha^{-1}, T_4—Electrostatic sprayer (3 mL L^{-1}) 150 L ha^{-1} and T_5—Non-electrostatic sprayer (3 mL L^{-1}) 150 L·ha^{-1}.

Conclusions

The introduction of electrically charged sprays in agricultural application has become inevitable for superior control on droplet transference with reduced drift and increased application efficiency with lesser spray chemical expenditure. This study on development of fully electric backpack type electrostatic spraying system could be a step forward in the area of indigenously developed modern plant protection equipment. The specific conclusions derived from the study were,

- The maximum CMR value (1.79 mC kg^{-1}) was observed at 9 kV charging electrode potential with an air assistance velocity of 10 m s^{-1} and nozzle discharge of 2 mL s^{-1} with the charging efficiency of 11.25 per cent of Rayleigh's charge limit (15.91 mC kg^{-1}).
- The number median diameter was (NMD) found to be 67 μm, which was when related to the VMD, resulted in the uniformity coefficient (U_C) of 0.73 and the relative span (R_S) of the spray spectrum of 0.61.
- There was approximately three-fold increment in overall canopy deposition occurred using electrostatically charged spray particles (350 deposits cm^{-2}) as compared to conventional spraying method (100 deposits cm^{-2}). The abaxial leaf surface deposition in case of charged spray was found to be decremented from upper (300–350 deposits cm^{-2}), middle (200–250 deposits cm^{-2}) to lower canopy (50–100 deposits cm^{-2}) leaves respectively.
- The water requirement for spraying per unit area was reduced to less than 1/3rd using electrostatic

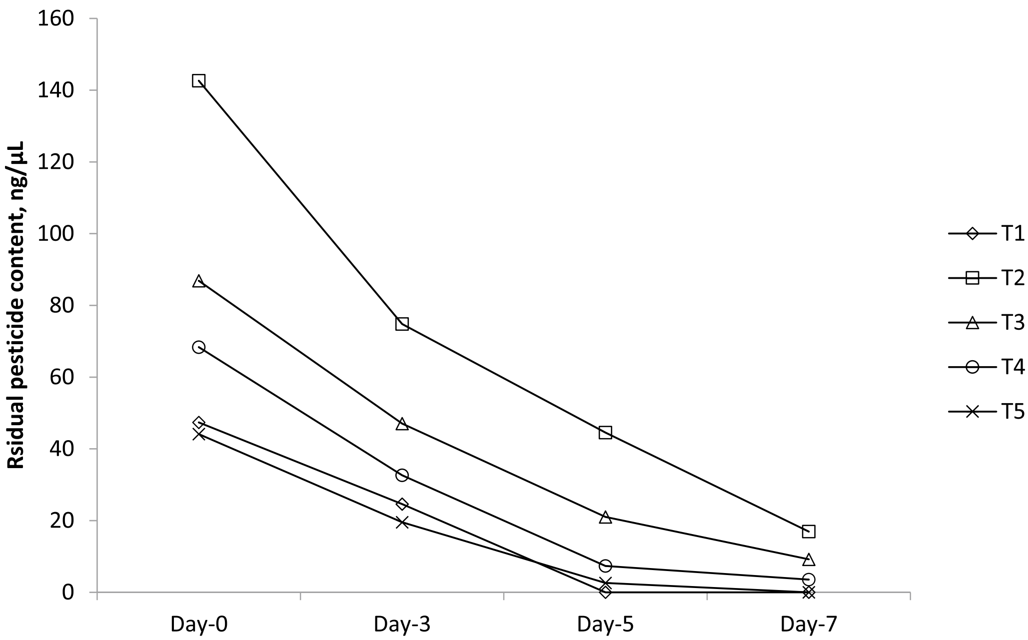

Fig. 12 Residual pesticide content w.r.t. day of application

spraying compared to conventional methods of agricultural spraying.

- The electrostatic spraying technique increased the deposition of active ingredient (147.63 ng μL^{-1}) by three-fold compared to the conventional sprayer (47.37 ng μL^{-1}) with the same dose of active ingredient per hectare.

Author contributions

DSK conceptualized, formed methodology, analysed and interpreted the experimental data regarding the development of electrostatic induction charging sprayer for agricultural applications. DD and SJP performed the review of the prior research and were major contributors in writing the manuscript. All authors read and approved the final manuscript.

Funding

Research Funding by Council for Scientific and Industrial Research (CSIR), New Delhi and Kerala Agricultural University, Thrissur.

Availability of data and materials

Will be made available on request.

Declarations

Ethics approval and consent to participate

All authors adhere to the scientific ethics and consent to participate.

Consent for publication

All authors consent to publish this original research article.

Competing interests

The authors declare that they have no competing interests.

Received: 20 December 2023 Accepted: 14 August 2024
Published online: 16 September 2024

References

Alamuhanna EA, Maghirang RG. Measuring the electrostatic charge of airborne particles. J Fd Agric Environ. 2010;8(3):1033–6.
Almekinders H, Ozkan HE, Reichard DL, Carpenter TG, Brazee RD. Spray deposition patterns of an electrostatic atomizer. Trans ASAE. 1992;36(6):1361–7.
Antuniassi UR, Velini ED, Oliviera RB, Maria AP, Figueiredo ZN. Systems of aerial spraying for soybean rust control. Eng Agric Jaboticabal. 2011;31(4):695–703.
Appah S, Wang P, Ou MX, Gong C, Jia WD. Review of electrostatic system parameters, charged droplets characteristics and substrate impact behavior from pesticides spraying. Int J Agric Biol Eng. 2019;12(2):1–9.
Asano K. Electrostatic Pesticide Spraying. In: Inculet II, Tanasescu FT, Cramariuc R, editors. The Modern Problems of Electrostatics with Applications in Environment Protection. Springer, Dordrecht: NATO Science Series; 1999.
Barbosa RN, Griffin JL, Hollier CA. Effect of spray rate and method of application in spray deposition. Appl Eng Agric ASABE. 2009;25(2):181–4.
Bode LE, Bowen HD. Spray distribution and charge-mass ratio of electrostatically charged agricultural sprays. Trans ASAE. 1991;34(5):1928–34.
Celen HI, Durgut MR, Gurkan GA, Erdal K. Effect of air assistance on deposition distribution of spraying by tunnel type sprayer. Afr J Agric Res. 2009;4(12):1392–7.
Choi JH, Byong JH, Park JS, Kim JH. Development of high voltage module for an electrostatic painting robot system. Int J Syst Appl Eng Dev. 2016;10:315–9.
Dwivedi CK, Daigavane MB. Multi-purpose low-cost DC high voltage generator (60 kV output), using Cockroft-walton voltage multiplier circuit. Int J Sc Technol Edu Res. 2011;2(7):109–19.
Esehaghbeygi A, Tadayyon A, Besharati S. Comparison of electrostatic and spinning-discs spray nozzles on wheat weeds control. J Am Sci. 2010;6(12):529–33.

Fritz BK, Parker C, Lopez JD, Hoffmann WC, Schleider P. Deposition and Droplet sizing characterization of a laboratory spray table. Appl Eng Agric, ASABE. 2009;25(2):175–80.
Gaunt L, Hughes J, Harrison N. Electrostatic deposition of charged insecticide sprays on electrically isolated insects. J Electrostatics. 2003;57(1):35–47. https://doi.org/10.1016/S0304-3886(02)00094-3.
Gil E, Llorens J, Landers A, Llop J, Giralt L. Field validation of DOSAVINA, ˜ a decision support system to determine the optimal volume rate for pesticide application in vineyards. Eur J Agron. 2011;35(1):33–46. https://doi.org/10.1016/j.eja.2011.03.005.
IPPC Secretariat. Scientific review of the impact of climate change on plant pests – A global challenge to prevent and mitigate plant pest risks in agriculture, forestry and ecosystems. Rome. FAO on behalf of the IPPC Secretariat. 2021. https://doi.org/10.4060/cb4769en
Jaworek A, Sobczyk AJ, Krupa A, Lackowski M, Czech T. Electrostatic deposition of nano-thin films on metal substrate. Bull Polish Sci. 2009;57(1):63–70.
Lane MD, Law SE. Transient charge transfer in living plants undergoing electrostatic spraying. Trans ASAE. 1982;25:1148–59.
Latheef M, Kirk IW, Carlton JB, Hoffmann WC. Aerial electrostatic charged sprays for deposition and efficacy against sweet potato whitefly (Bemisiatabaci) on cotton. Pest Mgmt Sci Wiley Interscience. 2008;65:744–52.
Law SE. Electrostatic induction instrument for tracking and charge measurement of airborne agricultural particulates. Trans ASAE. 1975; 40–47.
Law SE, Cooper SC. Depositional characteristics of charged and uncharged droplets applied by an orchard air carrier sprayer. Trans ASAE. 1988;31(4):984–9.
Law SE, Scherm H. Electrostatic application of a plant disease biocontrol agent for prevention of fungal infection through the stigmatic surfaces of blueberry flowers. J Electrostatics. 2005;63(5):399–408.
Lin Z, Xie J, Tian S, Wang X, Sun W, Mo X. Research and experiment of electrostatic spraying system for agricultural plant protection unmanned vehicle. Front Ecol Evol. 2023;11:1138180. https://doi.org/10.3389/fevo.2023.1138180.
Luciana N, Cramariuc R. Contribution about the electrohydrodynamic spraying. UPB Sci Bull Ser-C. 2009;71(3):205–13.
Magan N, Medina A, Aldred D. Possible climate-change effects on mycotoxin contamination of food crops pre and postharvest. Plant Pathol. 2011;60:150–63.
Mamidi V, Ghanashyam C, Patel MK, Reddy V, Kapur P. Electrostatic hand pressure swirl nozzle for small crop growers. Int J Appl Sci Tech Res Excellence. 2012;2(2):164–8.
Maynagh B, Ghobadian B, Johannama M, Hashjin T. Effect of electrostatic induction parameters on droplet charging for agricultural application. J Agric Sci Tech. 2009;11(1):249–57.
Mishra PK, Singh M, Sharma A, Sharma K, Singh B. Studies on effect of electrostatic spraying in orchards. Agric Eng Int J CIGR. 2014;16(3):60–9.
Oerke CN. Crop losses to pests. J Agric Sci. 2006;144(1):31–43.
Patel BM, Devmurari SH, Rathod MP. Development of high voltage solid state marx generator for liquid applications. Int J Eng Res Tech. 2014;3(12):755–8.
Patel MK, Sahoo HK, Nayak MK, Kumar A, Ghanashyam C, Amod K. Electrostatic nozzle: new trends in agricultural pesticide spraying. Int J Electr Electronics Eng. 2015; 6–11.
Petersen A. High power flyback, variable input-output voltage, decoupled power supply. United States Patent No. 4814965. 1989; https://patentimages.storage.googleapis.com/89/55/64/69ea52e2c933b9/US4814965.pdf
Robson S, Mauri MT, Fernandes HC, Monteiro PM, Rodrigues M, Cleyton BA. Parameters of electrostatic spraying and its influence on the application efficiency. Rev Ceres. 2013;60(4):474–9.
Salcedo R, Elena S, Zhu H, Fàbregas X, García-Ruiz F, Gil E. Evaluation of an electrostatic spray charge system implemented in three conventional orchard sprayers used on a commercial apple trees plantation. Crop Prot. 2023;167: 106212. https://doi.org/10.1016/j.cropro.2023.106212.
Savary S, Willocquet L, Pethybridge SJ, Esker P, McRoberts N, Nelson A. The global burden of pathogens and pests on major food crops. Nature Ecol Evol. 2019;3:430–9.
Sharma C, Jhala AK, Prajapati M. Low-cost high voltage generation: a technique. Int J Sci Eng Tech Res. 2015;4(12):4026–30.
Sundaraj R, Amuthavalli T, Vimala D. Invasion and establishment of the solanum whitefly Aleurothrixus trachoides (Back) (*Hemiptera: Aleyrodidae*) in South India. Curr Sci. 2018;115(1):29–31.
Sushil SN. Emerging issues of plant protection in India. Int Conf on Natural Res Management: Ecol Perspectives, SKUAST, Jammu. 2016.
Tong-Xian L, Philip AS, Conner JM. Evaluation of spray deposition on plant foliage with self-adhesive paper targets. Subtropical Plant Sci. 2004;36:39–43.
Van der Fels-Klerx HJ, Liu C, Battilani P. Modelling climate change impacts on mycotoxin contamination. World Mycotoxin J. 2016;9:717–26.
Waluyo S, Nugraha S, Permana Y. Miniature prototype design and implementation of modified multiplier circuit DC high voltage generator. Int J Electr Eng Tech. 2015;6(1):1–12.
Yu R, Zhou H, Zheng J. Design and experiments on droplet charging device for high range electrostatic sprayer. Pesticides in Modern World - Pesticide Use Mgmt. 2011; 137–148.
Zhou H, Ou M, Dong X, Zhou W, Dai S, Jia W. Spraying performance and deposition characteristics of an improved air-assisted nozzle with induction charging. Front Plant Sci. 2024. https://doi.org/10.3389/fpls.2024.1309088.

Publisher's Note